Journal of Advanced Sciences and Engineering Technologies (2026); 9(1):1-19

DOI: http://doi.org/10.32441/jaset.9.1.1

Journal of Advanced Sciences and Engineering Technologies

www.jasetj.com

Journal of Advanced Sciences and Eng. Technologies

JASET

Influence of Metakaolin-Based Self-Compacting Concrete on the Lateral Behavior of Exterior RC Joints

Harith Al-Salman *

Department of Architectural Engineering, College of Engineering, University of Babylon, Babylon, Iraq.

Keywords:

Reinforced concrete; Beam–column joints; Monotonic lateral loading; Ductility; Self-compacting concrete.

Highlights:

- Structural performance of full-scale exterior RC joints with metakaolin was tested.
- Metakaolin addition enhanced the peak lateral load capacity from 57.4 kN to 63.8 kN.
- Joint stiffness improved significantly from 1.45 kN/mm to 1.69 kN/mm.
- Cumulative energy dissipation increased from 1755 kN·mm to 1879 kN·mm.
- Metakaolin-based SCC led to gradual crack development and overall structural efficiency.

ARTICLE INFO

Article history:

Received	08 Jan	2026
Received in revised form	15 Mar	2026
Accepted	28 April	2026
Final Proofreading	05 May	2026
Available online	24 May	2026

Corresponding author:

Harith Al-Salman *

Department of Architectural Engineering, College of Engineering, University of Babylon, Babylon, Iraq.

Abstract: This study experimentally investigates the structural performance of exterior reinforced concrete beam–column joints incorporating metakaolin-based self-compacting concrete under monotonic lateral loading. Three full-scale exterior joint specimens with identical dimensions and reinforcement details were fabricated and tested under constant axial compression combined with progressively increasing lateral loading until failure. The experimental program focused on evaluating load-carrying capacity, stiffness, ductility, crack propagation, and energy dissipation behavior. The results demonstrated that the use of Metakaolin improved the structural response of the tested joints compared with the control specimen. The peak lateral load increased from 57.4 kN for the conventional specimen to 63.8 kN for the metakaolin specimen. In addition, stiffness improved from 1.45 to 1.69 kN/mm, while cumulative energy dissipation increased from 1755 to 1879 kN·mm. Crack development in the modified specimens progressed more gradually, with satisfactory deformation capacity maintained throughout the loading stages. The findings confirm that metakaolin-based self-compacting concrete can effectively enhance the strength, stiffness, and overall structural efficiency of exterior reinforced concrete joints.

INTRODUCTION

The beam–column joints are an important zone in reinforced concrete (RC) structures, where the forces of axial compression and tension, shear, bending moments and torsion are transferred from one structural member to another [1–3]. The behavior of these joints under seismic loading is complex due to multidirectional stress interactions between connected elements. Prior to the 1970s, seismic design requirements for beam–column joints were limited, and in many older RC structures, detailing was inadequate. These types of connections are therefore frequently found to lack adequate confinement, have poor shear resistance and are prone to brittle failure mechanisms during an earthquake [4, 5].

Based on the post-earthquake field investigation, the beam-column joints of the reinforced concrete frame structure are the most critical and most fragile parts of the structure, and they are the first to be damaged and even collapse when the structure is subjected to seismic action [6–9]. Research on failure mechanisms of joints [10, 11] shows that brittle shear failure can occur at the joint core when the shear strength is low, combined with a high concentration of stress. Buildings that meet current building codes can still exhibit poor failure modes because of construction or detailed design errors. Exterior joints, which are subject to lateral loading, are even more susceptible [12–14], and achieving adequate joint performance is one of the most critical aspects of seismic design and retrofit of an existing structure.

Several strengthening and retrofitting methods exist to address deficiencies in existing buildings. Many traditional techniques, such as reinforced concrete jacketing, shotcrete application, epoxy injection, and FRP systems, are effective in strengthening structural joints and increasing their stiffness [15–22]. Such methods, however, tend to have drawbacks such as increased structural mass, larger member dimensions, high labor requirements, and a complicated installation process [23, 24]. Thus, further research into more practical and efficient retrofit solutions is ongoing.

Different methods of strengthening joints have been studied recently, such as steel cages, prestressed steel angles, and stiffened steel plates, to increase joint confinement, ductility, and shear resistance. In this respect, steel plate retrofitting has attracted significant attention due to its minimal geometric modification and ease of

installation, thereby enhancing the structure's load-carrying capacity [16, 25, 26]. Mechanical characteristics of the existing concrete, particularly in the vicinity of congested joint areas, are also important factors affecting the efficiency of such retrofit systems.

Reinforced concrete structures have become more efficient and better behaved in construction due to improvements in concrete technology. Self-compacting concrete (SCC) is considered an effective alternative to conventional concrete, as it is highly flowable and requires no vibration to achieve full compaction [27, 28]. This property makes SCC an excellent material for highly reinforced areas, such as beam-column joints. Moreover, SCC can be used to increase filling ability, decrease internal voids, and increase the homogeneity, mechanical properties and durability of structural elements [29].

SCC's performance can be improved by adding supplementary cementitious materials; Among these, Metakaolin (MK) represents one of the most effective and promising. Metakaolin is produced by calcining kaolin clay at 650-900°C and is considered a highly reactive pozzolan [30, 31]. Furthermore, the product's fine particles, large specific surface area, and high levels of both amorphous silica and alumina make it highly reactive. Adding Metakaolin to SCC improves rheological properties (i.e., viscosity and cohesion), leading to less segregation/bleeding while maintaining proper flow [32, 33].

The high pozzolanic reactivity of Metakaolin increases the formation of calcium silicate hydrate gel, resulting in a denser microstructure and a refined pore structure in SCC, and it also improves the early-age performance of SCC [34]. Therefore, the durability and resistance to moisture, chloride ions and chemical attacks of SCCs with Metakaolin are better [30, 35]. Metakaolin was believed to be highly effective in improving the properties of self-compacting concrete compared with other additional cementitious materials. It is suitable for use in high-performance structural applications.

In addition to the performance benefits that a mechanically superior material would offer, Metakaolin can be used in the sustainable construction practice of replacing a portion of Portland Cement with Metakaolin, thereby reducing the carbon footprint associated with Portland Cement production [31]. As interest in environmentally friendly construction materials increases, metakaolin-based self-compacting concrete

(SCC) is being used more in new infrastructure projects. Hence, Metakaolin-reinforced or enhanced SCC is an ideal solution for critical load-bearing areas, such as beam-column joints, where performance and constructability are both important.

Although construction technology has advanced, few studies examine the performance of structures with beam–column joints under lateral loads when strengthened with metakaolin-based SCC. Most previous studies have concentrated on either material properties or joint behavior, with few studies combining both.

Previous studies have employed comprehensive finite element (FE) analysis to investigate the non-linear behaviour of reinforced concrete (RC) beam-column joints under various loading conditions. This study will provide useful data on the stress, crack, or failure mechanisms of beam-column joints. For many of the new cementitious materials (concrete treated with Metakaolin), however, testing is still necessary to determine their behavior under lateral pressure [11, 36, 37]. The behaviour of external beam-column junctions subjected to monotonic lateral loads has received less attention, particularly with respect to the effects of both SCC and strengthening.

Previous investigations of RC beam-column joints have primarily addressed conventional concrete and traditional reinforcement methods. There has also been relatively little exploration of how Metakaolin affects the structural performance of exterior RC joints under monotonic lateral loading. Given this gap in the literature, the purpose of this study is to investigate the contributions of using Metakaolin for enhancing the structural performance of exterior RC beam-column joints during lateral load testing. This will be done using controlled experimental methods.

PROGRAM FOR EXPERIMENTATION

Beam-column joint specimen design, dimensions, and reinforcing information

A section of a multi-story reinforced concrete building was represented by three external beam-column junction specimens, which were produced and tested. The total size of the specimens was determined by the capabilities and limitations of the testing facility at the University of Baghdad, Faculty of Engineering, Iraq. The exterior RC beam-column joints were cast using the geometric configuration depicted in Fig. 1.

Each beam had a length of 600 mm with a cross-sectional dimension of 210 × 200 mm, whereas the columns measured 250 × 200 mm in cross-section and 900 mm in height. Both beams and columns were reinforced longitudinally with 10 mm diameter bars and transversely with 6 mm diameter stirrups spaced 40 mm apart. The reinforcement detailing for all specimens was designed in accordance with the requirements of ACI 352R and ACI 318 [38, 39].

The University of Baghdad laboratory conducted tensile testing to determine the mechanical properties of 6 mm and 10 mm steel reinforcement bars. Table 1 summarizes the mechanical and physical properties of the reinforcement steel as defined by ASTM A615 standards [40]. The number of specimens was limited due to laboratory constraints and the high cost associated with full-scale beam–column joint testing.

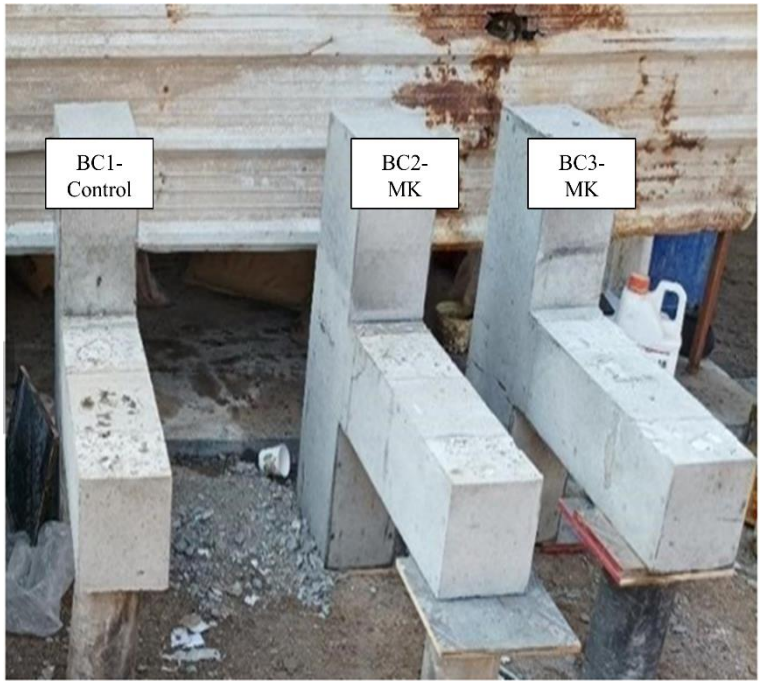

Fig. 1 Samples of BCJ

Table 1: Steel bars' physical characteristics

Bar diameter (mm)	Cross-sectional area (mm²)	Yield strength (MPa)	Tensile strength (MPa)	Maximum tensile strain (%)	Elastic modulus (GPa)
6	28.26	310	425	7.5	201
10	78.50	322	445	8.1	205

Materials and Mixture Proportions

Natural sand from Karbala, Iraq, with a bulk density of 1615 kg/m³ and a maximum nominal particle size of 4.75 mm, served as the fine aggregate (FA) in this study. The material's specific gravity is 2.60, its fineness modulus is 2.65, and its water absorption capacity is 2.41 percent. Conversely, the coarse aggregate (CA) was made of crushed gravel purchased from Baghdad, Iraq, with a unit weight of 1515 kg/m³ and a maximum nominal size of 9.5 mm.

A specific gravity of 2.50, a fineness modulus of 6.05, and a water absorption value of 1.75 percent were among its measured characteristics. Sieve analysis was carried out in compliance with ASTM C33 [41] to confirm adherence to standard requirements and guarantee material suitability.

The particle size distribution, which is essential for achieving the required fresh and hardened concrete performance, was determined using this method—the gradation curves for the FA and CA employed in this study are shown in Fig. 2.

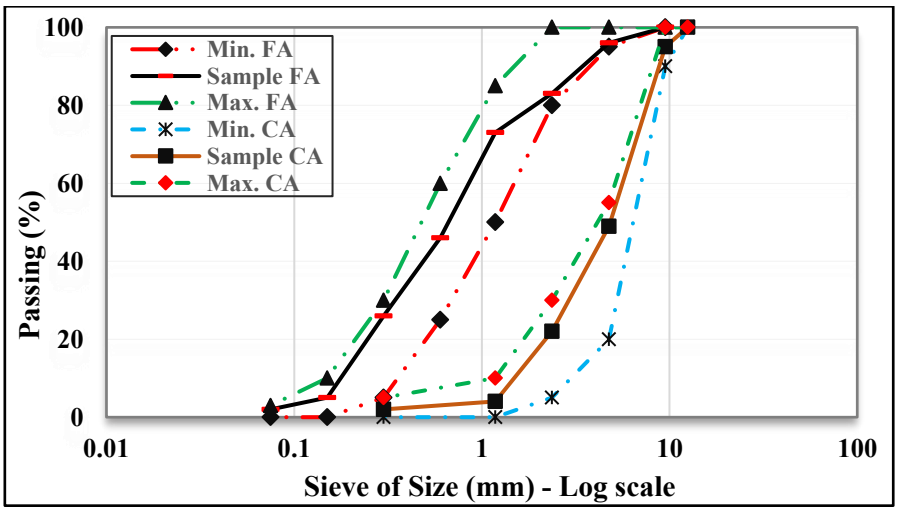

Fig. 2 Gradations of FA and CA

An X-ray fluorescence (XRF) spectrometer produced by Bruker (model S8 tiger) was utilized to investigate the chemical makeup of binders that were included in this study. Results indicated that Metakaolin (MK) exhibits a very large amount of aluminosilicate material (33% of total material), comprised primarily of silicon dioxide and aluminum oxide (<noise). Using X-ray diffraction (XRD) techniques, the phase composition of the sample was further investigated; XRD patterns obtained from samples collected in this study confirm that the phase composition of ordinary Portland cement (OPC) binders consists of calcium silicate compounds. In contrast, the phase compositions of metakaolin samples show significant amounts of quartz

(silica) and mullite (high-alumina silicate), as well as smaller quantities of hematite, anatase, and C3S.

The analysis also showed that Metakaolin contained a substantial quantity of aluminosilicate material; specifically, the total combined percentage of silicon oxide and aluminum oxide exceeded 97.81% (Table 2). This satisfies the ASTM C618-17 [42], which specifies that suitable pozzolanic materials must contain at least 70% of reactive aluminosilicate phases for use in cementitious and geopolymeric systems. Accordingly, Metakaolin is confirmed as a highly reactive supplementary binder suitable for enhancing cement-based composites.

Table 2 MK and OPC properties and chemical compositions

Compound	MK (wt%)	OPC (wt%)
SiO2	51.36	22.49
Al2O3	43.52	3.08
Fe2O3	1.25	3.25
CaO	0.83	64.71
MgO	0.99	1.05
SO3	1.07	1.96
Na2O	1.05	0.65
K2O	-	1.05
R2O *	0.05	1.34
TiO2	1.55	-
L.O.I.	2.4	0.39
Specific surface area (m^2/kg)	20,550	328
Density (g/cm3)	2.55	3.08

* R2O = Na2O + 0.658K2O

The specimens were cast using regular concrete manufactured in a lab with a compressive strength of 65 MPa. In this paper, the concrete mix design was based on ACI-211.1 [43]. The mix proportions for one cubic meter (m^3) of concrete are shown in Table 3. Three standard cylinders were used in laboratory experiments at the University of Babylon to determine these proportions. The average compressive strength of the cylindrical concrete specimens was 44.6 MPa, and the average tensile strength of three more cylinders was 2.0 MPa. Table 4 offers a thorough summary of the compressive and tensile strength values. In this study, ordinary Portland cement (OPC) Type I, complying with ASTM C150 [44], was obtained from Sulaymaniyah, Iraq. The water-to-cement (w/c) ratio was 0.33, and the proportions of binder, FA and CA in the concrete mix were 1:1.75:1.91.

At a 10% by weight, Metakaolin was added to replace cement partially. Throughout the process, drinking water fit for mixing concrete was used. In accordance with ASTM C494, the superplasticizer (SP) Master Glenium-54 was added to the mixture at a binder weight of 2%, improving workability while maintaining a low water content [45].

Table 3 Concrete mix proportions for 1 m³

	Ingredient	Quantity (kg/m³)
Designed Compressive strength (65) MPa	Cement	450
	Metakaolin	45
	Water	163
	W/C	0.33
	FA	870
	CA	950
	SP	9.9

Table 4: Tensile and compressive strengths of concrete cylinders

Samples	Density (kg/m3)	Average (kg/m³)	Compressive Strength (MPa)	Average (MPa)	Tensile Strength (MPa)	Average (MPa)
S.1	2389		63.9		2.05	
S.2	2401	2396	64.7	64.4	1.98	2.0
S.3	2399		64.6		1.97	

Loading Conditions: Methodology and Equipment

Members in moment-resisting frame structures subjected to lateral loading typically experience minimal moments at the beam mid-span; therefore, the adopted boundary conditions were designed to simulate realistic frame behavior, as illustrated in Fig. 3. In this setup, a roller support was used at the beam end. At the same time, the column base was restrained using a hinge support to permit rotation and prevent translational movement. The experimental program was conducted under a monotonic lateral loading procedure, as recommended by ACI T1.1 [46] and consistent with previous experimental programs [14, 47–51]. Due to the limited capabilities of the University of Kerbala's testing facilities, which could only be used under static loading, the current study chose static loading rather than cyclic loading, as employed in most previous studies to replicate seismic loading.

A hydraulic jack was first positioned at the top of the column, and the load was applied to the top in order to apply a constant axial load. A constant axial load of 110 kN (0.08*Ac* f′c) was applied throughout the test, and the lateral load was applied incrementally by placing a second hydraulic jack horizontally at the top of the column, with an eccentricity of about 70 mm from the column face. To assure lateral stability

during testing, the specimen was fixed with a rigid steel reaction frame. Axial deformation and realistic load-transfer behaviour were provided by a roller support placed above the specimen. Lateral loading was applied gradually to the column until failure, and load–displacement responses were recorded continuously by installing an LVDT at 70 mm from the column face, close to the loading point, which provided an accurate measurement of the horizontal movement.

Fig. 3 A picture of the loading technique specimen and prototype structure employed in the test setup

The EFNARC specifications [52] were used to test the fresh properties of self-compacting concrete (SCC), including slump flow, V-funnel, and L-box tests, which gauge SCC's flowability, passing ability, and deformability. Other tests, such as the J-ring test, were not adopted because they provide similar assessments and could lead to redundant testing.

RESULTS AND DISCUSSION

Peak Load Monotonic

The lateral loads at which the first crack was observed in the beam–column joints, the ultimate lateral load and the displacement at that moment are given in Table 5 as the main response parameters for the various exterior beam–column joints tested under monotonic loading. Given the same geometry, reinforcement, and loading conditions, the results indicated only slight differences in the load at which the crack initiates and at which the structure fails, with crack initiation loads varying by less than 28% and ultimate loads varying by approximately 16.2%.

Displacement responses at cracking and peak load stages were also very similar, confirming nearly identical stiffness among the specimens. Flexural cracks first appeared at the beam–column interface and progressively propagated toward the beam soffit as the lateral load increased. At ultimate load, cracks extended to the upper beam region, followed by concrete crushing and spalling near the beam compression zone, leading to a reduction in load-carrying capacity (Fig. 4). The specimens containing Metakaolin (MK) exhibited improved stiffness and load capacity due to the pozzolanic reaction, which enhanced the interfacial transition zone and produced additional C–S–H gel, resulting in a denser concrete matrix [33].

Table 5: Loads at the specimens' first crack and peak

Specimen designation	P_F (kN)	Displacement at first crack load, δ_F (mm)	P_p (kN)	Displacement at peak monotonic load, δ_P (mm)
BC1-Control	26	2.8	57.4	39.6
BC2-MK	22	3.2	61.3	37.6
BC3-MK	20	2.7	63.8	37.7

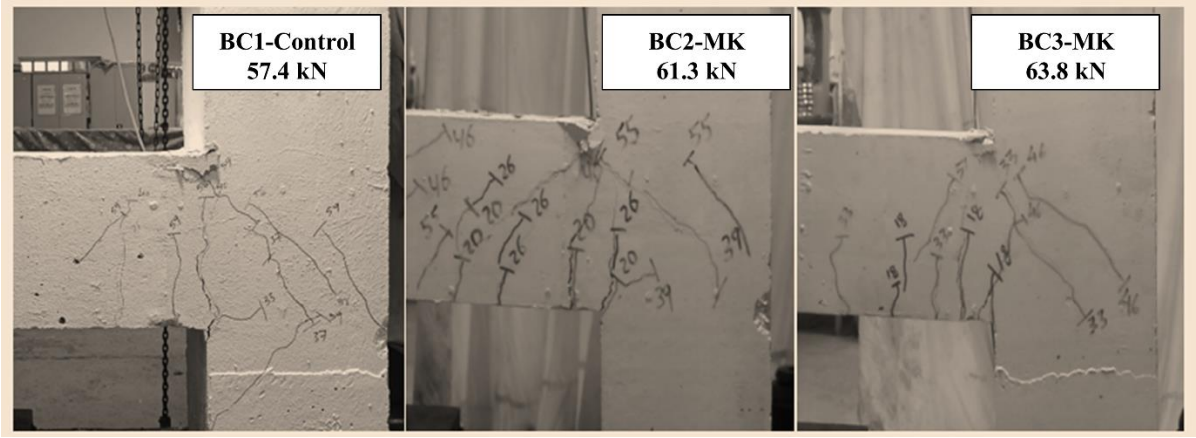

Fig. 4 Crack patterns in samples for testing

Curves of Load-Displacement

Fig. 5 shows the monotonic lateral loading-displacement response for all the beam-column joint specimens. A calibrated load cell and indicator system were used at a reference point 70 mm from the column face to record the critical failure values. In contrast, the applied load and associated displacement were continually monitored.

Initially, all the specimens showed an almost linear response, indicating that the structural behavior remained in the elastic range. As the lateral load increased gradually, microcracks began to form in the concrete cover, followed by progressive stiffness degradation of the concrete as the steel reinforcement reached yield. Continued loading led to the widening of cracks and the redistribution of internal

stresses, ultimately resulting in flexurally dominated failure of the beam–column joints at the final stage of testing.

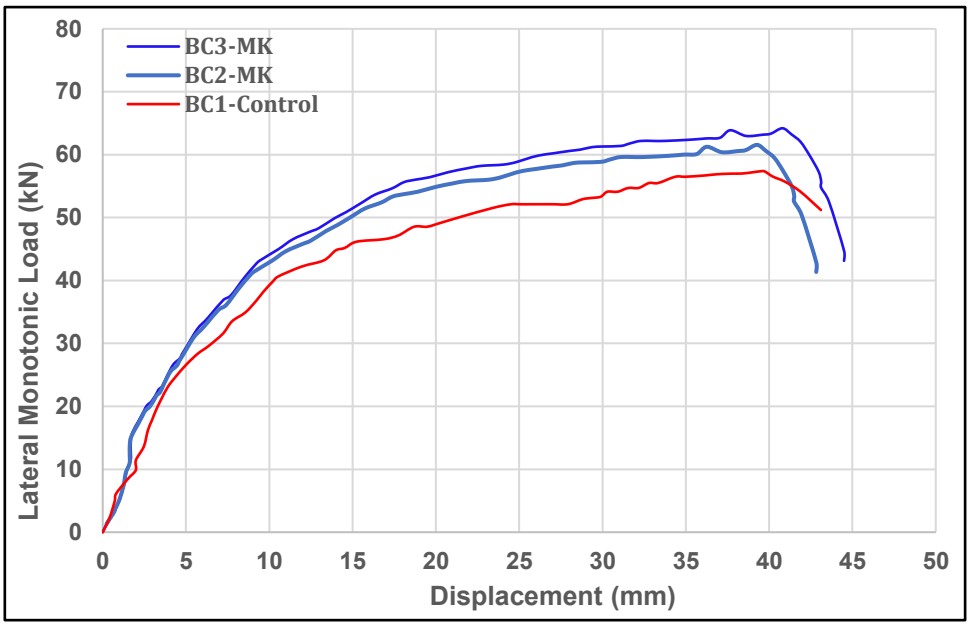

Fig. 5 Experimental specimen load-displacement curves

Stiffness and Energy Dissipation

Energy dissipation (E_{diss}) reflects the ability of exterior beam–column joints (BCJs) to absorb energy under lateral loading; higher values indicate greater resistance to structural damage [22, 51]. In this study, Ediss was calculated as the area under the monotonic load–displacement curve using the trapezoidal rule and Equation (1).

$$E_{diss} = \int_0^{\delta max} F(\delta).\, d\delta \approx \sum_0^{\delta_{i+1} = \delta max} \left(\left(\frac{F_{i+1} + F_i}{2} \right) x \left(\delta_{i+1} - \delta_i \right) \right) \qquad (1)$$

Equation (2) was used to calculate joint stiffness (K), which represents resistance to lateral deformation, as the ratio of the ultimate load to the corresponding displacement [53, 54].

$$\text{Stiffness (K)} = \frac{Pp}{\delta p} \qquad (2)$$

The results in Table 6 show that the energy dissipation values ranged from 1755 to 1879 kN·mm, with a variation of about 6.5%, while stiffness values ranged from 1.45 to 1.69 kN/mm, showing a variation of approximately 14.2%. Although energy dissipation is commonly evaluated under cyclic loading, the area under the monotonic load–displacement curve remains a reliable indicator of a specimen's energy absorption capacity.

Table 6: Results of experiments on the stiffness and energy dissipation of sampled

Samples designation	P_p (kN)	δ_P (mm)	E_{diss} (kN.mm)	K (kN/mm)
BC1-Control	57.4	39.6	1755	1.45
BC2-MK	61.3	37.6	1845	1.63
BC3-MK	63.8	37.7	1879	1.69

Stiffness and Energy Dissipation

The displacement ductility factor was adopted in this study to evaluate the ductility behavior of the specimens [54]. Based on the idealized bilinear load–displacement response, it was calculated using the ratio between the yield displacement and the effective ultimate displacement as per Equation (3) [25, 55].

$$\text{Ductility Factor } (\mu) = \frac{\delta_u}{\delta_y} \qquad (3)$$

Table 7: The specimens' ductility factor results

Sample designation	P_p (kN)	Yield of load, P_y (kN)	Yielding displacement, δy (mm)	Ultimate load, P_u (kN)	Effective ultimate displacement, δ_u (mm)	Ductility factor, μ
BC1-Control	57.4	44.7	12.6	48.8	45.8	3.6
BC2-MK	61.3	55.1	14.6	52.1	47.6	3.2
BC3-MK	63.8	55.8	14.9	54.2	46.4	3.1

where P_u (ultimate load) equals 85% * P_p

The yielding load (Py), yield displacement (δy), ultimate displacement (δu), peak load (Pp), and ductility factor (μ) of the tested specimens are shown in Table 7. The ductility factor varied by almost 16.1% between 3.1 and 3.6. The slightly reduced ductility of the Metakaolin (MK) specimens is explained by the concrete's denser microstructure and greater stiffness [5].

CONCLUSIONS

Based on the experimental investigation of three exterior reinforced concrete beam–column joints subjected to monotonic lateral loading, the following conclusions can be drawn:

- The tested specimens exhibited generally consistent structural behavior in terms of cracking load, ultimate load, stiffness, and energy dissipation, with peak loads ranging from 57.4 to 63.8 kN and a maximum variation of 16.2%.
- The incorporation of Metakaolin (MK) improved the load-carrying capacity of the joints, where specimen BC3-MK achieved an increase of approximately 11.1% compared with the control specimen.

- The load–displacement response showed an initial linear elastic behavior followed by stiffness degradation due to crack propagation and reinforcement yielding. Flexural cracks initiated near the beam–column interface and propagated toward the beam soffit and upper beam region with increasing load.
- Energy dissipation values ranged from 1755 to 1879 kN·mm, indicating improved energy absorption capacity for MK specimens and enhanced resistance to lateral loading.
- Stiffness values ranged from 1.45 to 1.69 kN/mm, with MK specimens demonstrating higher stiffness and greater resistance to lateral deformation.
- All specimens exhibited adequate ductility under monotonic loading, with ductility factors ranging from 3.1 to 3.6. Although the control specimen showed slightly higher ductility, MK specimens provided improved strength and stiffness.
- Flexural failure was the dominant failure mode in all specimens, characterized by concrete cracking and localized crushing near the beam–column joint region.
- Since the present study was limited to monotonic loading and a single MK replacement ratio, future work should examine cyclic loading behavior and different MK contents through both experimental and numerical investigations.

DATA AVAILABILITY STATEMENT

All data, models, and codes created and used in the course of this study are provided in the published article.

CONFLICTS OF INTEREST

The authors declare that there are no conflicts of interest, financial or personal, that could have influenced the research presented in this paper.

NOMENCLATURE

SCC	Self-Compacting Concrete
RC	Reinforced Concrete
MK	Metakaolin
FA	Fine Aggregate
CA	Coarse Aggregate
SP	Superplasticizer
P_F	First Crack Load
P_P	Peak Load
δ_F	Displacement at First Crack Load
δ_P	Displacement at Ultimate Load

E_{diss}	The energy dissipation
K	Stiffness
μ	Ductility factor

REFERENCES

[1] Chu, L., Tian, Y., Li, D., He, Y., & Feng, H. (2021). Shear behavior of steel reinforced concrete column-steel beam joints with or without reinforced concrete slab. Journal of Building Engineering, 35, 102063. https://doi.org/10.1016/j.jobe.2020.102063

[2] Abdelwahed, B. S., Kaloop, M. R., & El-Demerdash, W. E. (2021). Non-linear numerical assessment of exterior Beam-Column connections with Low-Strength concrete. Buildings, 11(11), 562. https://doi.org/10.3390/buildings11110562

[3] Jabbar, N. F., Owaid, A. M., & AL-Araji, A. M. (2025). STRUCTURAL BEHAVIOR OF ECO-EFFICIENT GEOPOLYMER CONCRETE BEAM–COLUMN JOINTS UNDER LATERAL MONOTONIC LOADING: THE IRAQI JOURNAL FOR MECHANICAL AND MATERIALS ENGINEERING. THE IRAQI JOURNAL FOR MECHANICAL AND MATERIALS ENGINEERING, 24(3), 72–95. https://doi.org/10.32852/8dxsa251

[4] Mosallam, A., Allam, K., & Salama, M. (2019). Analytical and numerical modeling of RC beam-column joints retrofitted with FRP laminates and hybrid composite connectors. Composite Structures, 214, 486–503. https://doi.org/10.1016/j.compstruct.2019.02.032

[5] Moradi, R., Alazam, R., Alaaraje, H. M., Owaid, A. M., & Jabbar, N. F. (2026). Numerical study of a new frictional damper for vibration control of different hazard levels and its comparison with friction-rotational damper in reinforced concrete frames. Journal of Building Pathology and Rehabilitation, 11(2), 146. https://doi.org/10.1007/s41024-026-00820-y

[6] Tavasoli, E., Rezaifar, O., & Kheyroddin, A. (2022). Seismic performance of RC joints retrofitted by external diagonal bolts. Journal of Building Engineering, 46, : 103691. https://doi.org/10.1016/j.jobe.2021.103691

[7] Vecchi, F., & Belletti, B. (2021). Capacity assessment of existing RC columns. Buildings, 11(4), 161. https://doi.org/10.3390/buildings11040161

[8] Alih, S. C., & Vafaei, M. (2019). Performance of reinforced concrete buildings and wooden structures during the 2015 Mw 6.0 Sabah earthquake in Malaysia. Engineering Failure Analysis, 102, : 351-368.

https://doi.org/10.1016/j.engfailanal.2019.04.056

[9] Ates, S., Kahya, V., Yurdakul, M., & Adanur, S. (2013). Damages on reinforced concrete buildings due to consecutive earthquakes in Van. Soil Dynamics and Earthquake Engineering, 53, 109-118. https://doi.org/10.1016/j.soildyn.2013.06.006

[10] Qasem, M., Hasan, M., Muhamad, R., & Mutafi, A. (2022). Non-linear 3D finite element analysis of precast reinforced concrete Beam-Column joint under monotonic static load. Materials Today: Proceedings, 65, 746–757. https://doi.org/10.1016/j.matpr.2022.03.284

[11] Qasem, M., Hasan, M., & Muhamad, R. (2023). Finite element simulation of precast moment resisting reinforced concrete beam-column joint subjected to monotonic load. Materials Today: Proceedings. https://doi.org/10.1016/j.matpr.2023.03.532

[12] Duan, H., & Hueste, M. B. D. (2012). Seismic performance of a reinforced concrete frame building in China. Engineering Structures, 41, 77-89. https://doi.org/10.1016/j.engstruct.2012.03.030

[13] Chung, L.-L., Chen, Y.-T., Sun, C.-H., Lien, K.-H., & Wu, L.-Y. (2012). Applicability investigation of code-defined procedures on seismic performance assessment of typical school buildings in Taiwan. Engineering structures, 36, : 147-159. https://doi.org/10.1016/j.engstruct.2011.12.001

[14] Owaid, A. M., Akhaveissy, A. H., & Al-Abbas, B. H. (2026). Retrofitting Seismically Designed Exterior Beam-Column Joints under Lateral Monotonic Loading: A Numerical Analysis Based on Experimental Testing. Journal of Rehabilitation in Civil Engineering, 14(1), 2043. https://doi.org/10.22075/jrce.2024.33704.2043

[15] Tsonos, A.-D. G. (2010). Performance enhancement of R/C building columns and beam–column joints through shotcrete jacketing. Engineering Structures, 32(3), 726–740. https://doi.org/10.1016/j.engstruct.2009.12.001

[16] Torabi, A., & Maheri, M. R. (2017). Seismic repair and retrofit of RC beam–column joints using stiffened steel plates. Iranian Journal of Science and Technology, Transactions of Civil Engineering, 41, : 13-26. https://doi.org/10.1007/s40996-016-0027-y

[17] Hung, C.-C., Hsiao, H.-J., Shao, Y., & Yen, C.-H. (2023). A comparative study on the seismic performance of RC beam-column joints retrofitted by ECC, FRP, and concrete jacketing methods. Journal of Building Engineering, 64, : 105691.

https://doi.org/10.1016/j.jobe.2022.105691

[18] Wahab, A. G., Zhong, T., Wei, F., Hakimi, N., & Ahiwale, D. D. (2024). Seismic performance enhancement of RC framed structures through retrofitting and strengthening: An experimental and numerical study. Asian Journal of Civil Engineering, 25(1), 555–573. https://doi.org/10.1007/s42107-023-00794-z

[19] Khodaei, M., Saghafi, M. H., & Golafshar, A. (2021). Seismic retrofit of exterior beam-column joints using steel angles connected by PT bars. Engineering Structures, 236, : 112111. https://doi.org/10.1016/j.engstruct.2021.112111

[20] Maddah, A., Golafshar, A., & Saghafi, M. H. (2020). 3D RC beam–column joints retrofitted by joint enlargement using steel angles and post-tensioned bolts. Engineering Structures, 220, : 110975. https://doi.org/10.1016/j.engstruct.2020.110975

[21] Karayannis, C. G., & Sirkelis, G. M. (2008). Strengthening and rehabilitation of RC beam–column joints using carbon-FRP jacketing and epoxy resin injection. Earthquake Engineering & Structural Dynamics, 37(5), 769–790. https://doi.org/10.1002/eqe.785

[22] Owaid, A. M., & Akhaveissy, A. H. (2026). Experimental and numerical study on retrofitting partially damaged exterior beam-column joints under lateral monotonic loading. World Journal of Engineering, 1–23. https://doi.org/10.1108/WJE-05-2025-0317

[23] Karayannis, C. G., Chalioris, C. E., & Sirkelis, G. M. (2008). Local retrofit of exterior RC beam–column joints using thin RC jackets—An experimental study. Earthquake Engineering & Structural Dynamics, 37(5), 727–746. https://doi.org/10.1002/eqe.783

[24] Pohoryles, D. A., Melo, J., Rossetto, T., Varum, H., & Bisby, L. (2019). Seismic retrofit schemes with FRP for deficient RC beam-column joints: State-of-the-art review. Journal of Composites for Construction, 23(4), 3119001. https://doi.org/10.1061/(ASCE)CC.1943-5614.0000950

[25] Deng, B.-Y., Liu, X., Yu, K.-Q., Li, L.-Z., & Chen, Y. (2022). Seismic retrofitting of RC joints using steel cage and haunch with bolted steel plate. Structures, 43, : 285-298. https://doi.org/10.1016/j.istruc.2022.06.056

[26] Campione, G., Cavaleri, L., & Papia, M. (2015). Flexural response of external RC beam–column joints externally strengthened with steel cages. Engineering Structures, 104, : 51-64. https://doi.org/10.1016/j.engstruct.2015.09.009

[27] Shi, C., Wu, Z., Lv, K., & Wu, L. (2015). A review on mixture design methods for self-compacting concrete. Construction and Building Materials, 84, 387–398. https://doi.org/10.1016/j.conbuildmat.2015.03.079

[28] Vivek, S. S., & Dhinakaran, G. (2017). Durability characteristics of binary blend high strength SCC. Construction and Building Materials, 146, 1–8. https://doi.org/10.1016/j.conbuildmat.2017.04.063

[29] Dadsetan, S., & Bai, J. (2017). Mechanical and microstructural properties of self-compacting concrete blended with Metakaolin, ground granulated blast-furnace slag and fly ash. Construction and Building Materials, 146, 658–667. https://doi.org/10.1016/j.conbuildmat.2017.04.158

[30] Vejmelková, E., Keppert, M., Grzeszczyk, S., Skaliński, B., & Černý, R. (2011). Properties of self-compacting concrete mixtures containing metakaolin and blast furnace slag. Construction and Building Materials, 25(3), 1325–1331. https://doi.org/10.1016/j.conbuildmat.2010.09.012

[31] Kavitha, O. R., Shanthi, V. M., Arulraj, G. P., & Sivakumar, V. R. (2016). Microstructural studies on eco-friendly and durable Self-compacting concrete blended with Metakaolin. Applied Clay Science, 124–125, 143–149. https://doi.org/10.1016/j.clay.2016.02.011

[32] Nadeem, A., Memon, S. A., & Lo, T. Y. (2014). The performance of Fly ash and Metakaolin concrete at elevated temperatures. Construction and Building Materials, 62, 67–76. https://doi.org/10.1016/j.conbuildmat.2014.02.073

[33] Owaid, A. M., Jabbar, N. F., Owaid, H. M., & Al-Abbas, B. H. (2026). Comprehensive mechanical, durability, and microstructural assessment of lightweight GGBS–metakaolin geopolymer concrete incorporating LECA. Construction and Building Materials, 506, 144961. https://doi.org/10.1016/j.conbuildmat.2025.144961

[34] Ghoddousi, P., & Adelzade Saadabadi, L. (2017). Study on hydration products by electrical resistivity for self-compacting concrete with silica fume and Metakaolin. Construction and Building Materials, 154, 219–228. https://doi.org/10.1016/j.conbuildmat.2017.07.178

[35] Melo, K. A., & Carneiro, A. M. P. (2010). Effect of Metakaolin's finesses and content in self-consolidating concrete. Construction and Building Materials, 24(8), 1529–1535. https://doi.org/10.1016/j.conbuildmat.2010.02.002

[36] Alshaikh, I. M. H., Nehdi, M. L., & Abadel, A. A. (2024). Numerical investigations on progressive collapse of rubberized concrete frames

strengthened by CFRP sheets. Structures, 60, 105918. https://doi.org/10.1016/j.istruc.2024.105918

[37] Koutromanos, I. (2011). *Numerical analysis of masonry-infilled reinforced concrete frames subjected to seismic loads and experimental evaluation of retrofit techniques*. University of California, San Diego.

[38] John F. Bonacci, S. M. A. (2002). Recommendations for Design of Beam-Column Connections in Monolithic Reinforced Concrete Structures. American Concrete Institute, ACI 352R-02, 1–37.

[39] Farmington Hills, MI, U. (2019). Building Code Requirements for Structural Concrete and Commentary. American Concrete Institute, ACI 318-19, 628.

[40] ASTM A615/AM615-15. (2015). Standard Specification for Deformed and Plain Carbon-Steel Bars for Concrete Reinforcement. American Society for Testing and Materials.

[41] ASTM C33/C33M-16. (2016). Standard specification for concrete aggregate. American Society for Testing and Materials.

[42] ASTM 618/C618-17. (2017). Standard Specification for Coal Fly Ash and Raw or Calcined Natural Pozzolan for Use in Concrete. American Society for Testing and Materials.

[43] Dixon, Donald E., Jack R. Prestrera, George RU Burg, Subcommittee A. Chairman, Edward A. Abdun-Nur, Stanley G. Barton, L. W. B. et al. (1991). Standard Practice for Selecting Proportions for Normal, Heavyweight, and Mass Concrete. American Concrete Institute (ACI 211.1-91). (1991, Reapproved 2002).

[44] ASTM C150/C150-07. (2007). Standard Specification for Portland Cement. American Society for Testing and Materials.

[45] ASTM C494/C494-05. (2005). Standard specification for chemical admixtures for concrete. American Standard for Testing and Materials; West Conshohocken, Pennsylvania, USA.

[46] Norman L. Scott NMH, Michael E. Kreger, L. D. M. (2001). Commentary on Acceptance Criteria for Moment Frames Based on Structural Testing. American Concrete Institute, ACI T1.1-01.

[47] Azimi, M., Adnan, A. Bin, Bin Mohd Sam, A. R., Tahir, M. M., Faridmehr, I., & Hodjati, R. (2014). Seismic performance of RC beam-column connections with continuous rectangular spiral transverse reinforcements for low ductility classes. The Scientific World Journal, 2014(1), 802605.

https://doi.org/10.1155/2014/802605

[48] Alhaddad, M. S., Siddiqui, N. A., Abadel, A. A., Alsayed, S. H., & Al-Salloum, Y. A. (2012). Numerical investigations on the seismic behavior of FRP and TRM upgraded RC exterior beam-column joints. Journal of Composites for Construction, 16(3), 308–321. https://doi.org/10.1061/(ASCE)CC.1943-5614.0000265

[49] Melo, J., Varum, H., & Rossetto, T. (2022). Experimental assessment of the monotonic and cyclic behaviour of exterior RC beam-column joints built with plain bars and non-seismically designed. Engineering Structures, 270, 114887. https://doi.org/10.1016/j.engstruct.2022.114887

[50] Wang, Z., Huang, J., Chang, Z., & Lu, Y. (2022). Experimental and Numerical Investigation on Seismic Performance of RC Exterior Beam-Column Joints with Slabs. Shock and Vibration, 2022(1), 3679431. https://doi.org/10.1155/2022/3679431

[51] Melo, J., Pohoryles, D. A., Rossetto, T., & Varum, H. (2021). Full-scale cyclic testing of realistic reinforced-concrete beam-column joints. MethodsX, 8, : 101409. https://doi.org/10.1016/j.mex.2021.101409

[52] Bibm C, E. E. (2005). EFNARC: The European guidelines for self compacting concrete. Specification, Production and Use, 63(3).

[53] Ugale, A. B., & Khante, S. N. (2020). Study of energy dissipation of reinforced concrete beam-column joint confined using varying types of lateral reinforcements. Materials Today: Proceedings, 27, 1356–1361. https://doi.org/10.1016/j.matpr.2020.02.690

[54] Sakthimurugan, K., & Baskar, K. (2021). Experimental investigation on rcc external beam-column joints retrofitted with basalt textile fabric under static loading. Composite Structures, 268, : 114001. https://doi.org/10.1016/j.compstruct.2021.114001

[55] Park, R. (1989). Evaluation of ductility of structures and structural assemblages from laboratory testing. Bulletin of the new Zealand society for earthquake engineering, 22(3), 155–166. https://doi.org/10.5459/bnzsee.22.3.155-166